

# Brain Tumor Segmentation and Classification in Mr Images Using Residual U-Net Semantic Segmentation Model

Murali Krishna Atmakuri<sup>1</sup>, A. Ganesh Ram<sup>2</sup>, V.V.K.D.V. Prasad<sup>3</sup>

Submitted:10/03/2024    Revised: 25/04/2024    Accepted: 02/05/2024

**Abstract:** Brain tumor identification makes use of machine learning and computer vision methods in order to automatically identify and categorize brain cancers in medical images such as MRI scans. A model for the segmentation and identification of brain tumors based on a residual U-Net is proposed in this work. The Residual U-Net is an altered variant of the U-Net architecture that is used in semantic segmentation tasks. It incorporates the concept of residual connections, which allows for the model to learn more complex representations of the input data and can result in more accurate segmentation. Residual connections allow for deeper networks to be trained while mitigating the vanishing gradient problem. This resulted in accurate segmentation of brain tumors, particularly in cases where the tumors are small or located in complex regions of the brain. The proposed model obtained a higher tversky of 0.89 and higher PSNR of 30.

**Keywords:** Brain tumor stage classification, CNN model, Residual U-Net, Segmentation, Tversky

## 1. Introduction

A brain tumor is an abnormal development of cells in the brain, and depending on its nature, it may or may not be cancerous. Every area of the brain is susceptible to the development of tumors, which may disrupt the normal functioning of the brain. Headaches, seizures, nausea and vomiting, trouble speaking or seeing, and changes in mood or personality are some of the frequent symptoms of a brain tumor. The symptoms of a brain tumor might vary depending on its location and size, but these are some of the more common ones [1].

The severity of the risks posed by a brain tumor is directly proportional to factors such as the tumor's kind, location, size, and pace of development. Although some brain tumors develop at a relatively modest rate and respond well to treatment with surgery or radiation therapy, others are more aggressive and pose a greater risk of death. It may be more challenging to treat malignant brain tumors if the cancer has migrated to other sections of the body. Malignant brain tumors may also spread to other parts of the body. Having a brain tumor is a significant medical disease that has to be diagnosed and treated as soon as possible. It is essential that you get the advice and diagnosis of a qualified medical practitioner if you are having any symptoms that you suspect may be caused by a brain tumor [2].

According to the Indian Council of Medical Research (ICMR), the annual incidence rate of brain tumors in India

is believed to be somewhere in the range of three to four cases per one hundred

thousand persons. There are around 40,000 new instances of brain tumors diagnosed in India each year. Brain tumors account for approximately 2% of all malignancies diagnosed in the country. In India, brain tumors are the tenth most frequent kind of cancer, and males are more likely than women to be diagnosed with the condition. The occurrence of brain tumors in India is age-dependent, with the greatest rates being observed in adults between the ages of 50 and 70 years old. In addition, the incidence of brain tumors is much greater in certain parts of India compared to other parts, which may be the result of environmental factors [3].

The Magnetic Resonance Imaging (MRI) method is one of the most frequent imaging procedures used in modern medicine. This method creates comprehensive pictures of the interior of the body, including the brain, by combining a powerful magnetic field with radio waves. Since it is able to provide very precise pictures of the brain tissue, magnetic resonance imaging (MRI) is especially beneficial for the detection of brain tumors. These images enable medical professionals to see irregularities that may be symptoms of a tumor. During an MRI scan of the brain, many pictures are taken from a variety of perspectives, and then these images are merged to provide a three-dimensional representation of the brain. The pictures obtained from the MRI may offer information about the size, location, and kind of the tumor, in addition to the information regarding the surrounding brain tissue [4]. This information is essential for directing treatment choices, such as determining whether the tumor should be removed surgically or if radiation therapy should be used

<sup>1</sup> Annamalai University, Annamalainagar-608002, India  
ORCID ID : 0000-0001-5957-2554

<sup>2</sup> Madras Institute of Technology, Anna University, Chennai-600025, India

<sup>3</sup> Gudlavalluru Engineering College, Gudlavalluru-521356, India

\* muralikrishna.atmakuri80@gmail.com

to treat it. The progression of brain tumors over time, as well as their reactions to therapy, may both be tracked with the use of MRI. The physicians are able to follow changes in the tumor size and composition by repeatedly scanning it using an MRI machine. This may assist in determining whether or not the therapy is successful.

One area of research that is now being conducted in the field of medical image analysis is the use of deep learning to the automated diagnosis of brain tumors. In the detection of brain cancers in medical imagery such as MRI scans, deep learning algorithms such as convolutional neural networks (CNNs) have shown encouraging results. In most cases, there is more than one phase involved in the process of applying deep learning to automatically identify brain tumors. The intensity of the medical pictures is first normalized, and then image noise is minimized as part of the pre-processing step. After that, the images that have been pre-processed are placed into a deep learning model that is comprised of labeled images. This procedure takes place after the images have been fed into the model.

Throughout the course of its training, the deep learning model acquires the knowledge necessary to extract pertinent characteristics from medical pictures and to categorize the extracted features according to a variety of criteria, such as normal brain tissue or cancerous tissue. After the model has been trained, it can be used to automatically identify fresh medical photos as either normal or as harboring a brain tumor [5]. This can be done even if the images have never been seen before. Deep learning has the potential to increase the accuracy and speed of diagnosis, as well as minimize the need for radiologists to manually interpret medical pictures. Automated brain tumor identification might also reduce the requirement for human interpretation of medical images. Nevertheless, in order for these strategies to be extensively used in clinical practice, further research and validation will need to be conducted. .

This paper presents a deep learning based segmentation and detection model to identify the tumor in brain MRI images. Section I presented the introduction to the paper. Section II presents the literature carried out in the field of research. The Third section presents the proposed model followed by experimental results and conclusion

## 2. Literature

N. Arunkumar et al. [6] presented a technique for the segmentation of brain tumors that identifies at least three important areas for the expansion of future research. K-means clustering will be used as an element of the main organization in the process of improving the MR image so that it can be marked in distinct regions depending on the grayscale of their own specific areas. This will be the first step. This will be done. Second, artificial neural networks

are used to choose the appropriate item for the training phase. Finally, the division step will include the extraction of the textural features of the region affected by the brain tumour. When it comes to determining the nature of a brain tumour, the grayscale characteristics of the tumour are examined and used in the diagnosis process. This allows for the brain tumour to be classified as either benign or malignant.

Mansi Lather et al [7] discussed the many approaches of segmentation that are currently accessible. The work that was done by a large number of researchers in the past to partly or totally automate the task of segmenting the brain tumour is the primary subject of this article. The specifics of the compiled information from the research that was looked at have been tallied. The clinical adoption of a given segmentation approach is determined by how simple the method is and how much human supervision it requires.

C. Jaspin Jeba Sheela et al [8] proposed a method that combines morphological operation, region growing, and region of interest (ROI) (Dilation and Erosion). This technique first determines the roughly growing region (RG). Pixels are grouped into bigger areas via a process called "region growth" that begins at the seed locations. In noisy pictures where edges are hard to identify, region growth based approaches perform better than edge based techniques. The input picture undergoes morphological edge detection, and the image is then enhanced by reconstructing it via erosion and dilation. The suggested work is broken down into three sections: preprocessing to lower noise, fuzzy C-Means for region growth, and morphological edge recognition for picture enhancement. Consequently, the identification of morphological edges may be divided into two groups: dilation and erosion. To obtain the output, use the Gaussian filter last. Following that, the tumour from the brain MRI image is detected and segmented using Fuzzy C-Means clustering (FCM), seeded area expanding, and afterwards.

Tanber Hasan Shemanto et al [9] presented a thresholding method, in order to get rid of brain tumours in 2D magnetic resonance brain pictures (MRI). For the purpose of preprocessing MRI data, the authors advised using a HOFILTER. This filter filters out unwanted noise and gets the image ready for tumour segmentation. When they compared the results to those of other studies on segmentation and detection, they found that ours were superior for a range of approaches. This led us to conclude that the methodology was superior.

M. Mohammed Thaha et al [10] developed Enhanced Convolutional Neural Networks (ECNN) is a technique for automated segmentation. This approach optimises the loss function using the BAT algorithm. The fundamental objective of this study is to offer an optimization-based

approach to the segmentation of MRIs. A deep architecture can be designed since small kernels allow for it. It has a beneficial effect with regard to overfitting provided that the network is given the lighter weights to use. At the pre-processing stage, methods for skull stripping and picture enhancement are used.

Zhihua Liu et al [11] provided the survey with an in-depth analysis of newly established strategies for segmenting brain tumours using deep learning. This study selects and discusses approximately 150 scholarly publications, delving deeply into topics concerning technical issues such like network architecture design, segmentation under unbalanced situations, and multi-modality processes. In addition to this, the authors facilitate meaningful conversations around the potential future routes of growth.

Javeria Amin et al [12] described an innovative approach to the diagnosis of tumours. The malignant and benign tumour instances are correctly segmented and classified by the architecture that has been provided. Many different techniques from the spatial domain are used in order to improve and precisely segment the input photos. Additionally, both Alex and Google networks are employed for classification, and as a consequence, two score vectors are produced after the softmax layer. The two score vectors are also concatenated before being sent into a variety of classifiers and the softmax layer.

Sourodip Ghosh et al [13] utilized a modified version of the U-Net that uses VGG-16 (tumor cells) to segment brain MRI images as well as locate regions of interest. By evaluating the TCGA-LGG dataset (3929 pictures) from the TCI repository, the authors compare the results of enhanced U-Net with a custom-designed U-Net architecture. They get pixel levels of accuracy of 0.994 as well as 0.9975 from basic U-Net as well as enhanced U-Net designs, respectively.

R.Thillaikarasi et al [14] provided an innovative deep learning approach (kernel based CNN with M-SVM) to automatically and effectively segment the tumour. The processes in the study that is being presented include preprocessing, feature extraction, picture classification, and brain tumour segmentation. The Laplacian of Gaussian filtering technique (LoG) and Contrast Limited Adaptive Histogram Equalization (CLAHE) are used to improve and smooth the MRI image, and features may be derived from it depending on the location, shape, and surface properties of the tumour in the brain. In accordance with the chosen characteristics, M-SVM is used to classify the images. With the aid of the kernel-based CNN approach, the tumour is segmented from the MRI picture.

Shiv Naresh Shivhare et al [15] offered a two-stage, automated system for brain tumour segmentation. Using the convex hull technique, a rough assessment of the brain

tumour is done in the first step. By using the derived coarse estimate as the active contour model's initialization in the subsequent step, the necessity for human involvement is removed. In order to find high-energy areas and build convex hulls over the chosen important locations, multiscale Harris energy is calculated at various levels. This process helps to discover abnormalities in the input MR images.

### 3. Proposed model

The act of dividing an image into several segments or areas, each of which corresponds to a distinct item or component of the picture, is known as image segmentation. A convolutional neural network (CNN) model for image segmentation begins with an input image and produces a segmentation map, where each pixel in the map corresponds to a segment or area in the original image. Using a labeled dataset of input images and associated segmentation maps, the goal is to train the model to an accuracy level that minimizes the difference between the predicted and the actual segmentation map. After training is finished, the model may be used to the segmentation of new images that weren't included in the training set.

#### 3.1 U-Net image segmentation

Image segmentation tasks make frequent use of the well-known U-Net neural network design, which is often used for this purpose. Since the design of the network is shaped like the letter "U," it was given the name "U-Net" to reflect this resemblance. The encoder and the decoder make up the U-Net architecture. The encoder increases the quantity of feature maps while progressively reducing the spatial resolution of the input picture. The decoder reduces the amount of feature maps while progressively restoring the original spatial resolution.

The following is an operation by breakdown of a typical U-Net architecture:

1.Encoder: The encoder is made up of a number of convolutional layers, which are then followed by a downsampling procedure that brings the feature maps' spatial resolution to a lower level. Both max pooling and strided convolution are viable options for doing the downsampling procedure. In each subsequent phase in the downsampling process, the number of feature maps generally increases by a factor of two.

2.The bottleneck is a portion of the network that is located in the center and has a lower spatial resolution than both the encoder and the decoder. It is made up of many convolutional layers that are responsible for extracting high-level characteristics from the picture that is fed into it.

3.Decoder: The decoder is comprised of a sequence of upsampling operations that progressively regain the

original spatial resolution of the input picture while simultaneously lowering the number of feature mappings. The upsampling procedure may be accomplished via the use of either interpolation or transposed convolution. In each subsequent phase in the upsampling process, the number of feature maps is generally cut in half.

4. Skip connections: The U-Net design also features skip connections, which link the encoder and the decoder while maintaining the same spatial resolution. The decoder is granted access to high-level information of the encoder as a result of the skip connections. These features are vital to proper segmentation. In most cases, the skip connections may be obtained by concatenating the feature maps obtained from the encoder with those obtained from the layer of the associated decoder.

5. Output: The U-Net algorithm produces a segmentation map as its final output, and this map has the same level of spatial resolution as the original picture. Convolutional layers with sigmoid activation functions are used to produce the segmentation map. This function outputs a probability value for each pixel in the input picture. The map is built utilizing these functions.

While training the U-Net architecture, a cross-entropy loss function may be used. This function does a comparison between the predicted segmentation map and the actual ground truth segmentation map. It is possible to optimize the weights of the network by making use of stochastic gradient descent or one of the other available optimization methods.

### 3.2 Residual U-Net

A deep learning architecture called Residual U-Net was created by combining the ideas presented in the U-Net and ResNet models of architecture. The U-Net design is often used for image segmentation tasks, while the ResNet architecture was created to help address the problem of fading gradients in very deep neural networks. Both of these architectures are frequently employed. When residual connections are introduced to the U-Net design, as they are in a Residual U-Net, this makes it possible for information to move directly across various levels. This makes it possible to train the network more efficiently and helps to alleviate the issue of disappearing gradients.

The design of the Residual U-Net is made up of two different paths: a shrinking route and an expanding one. The contracting route is made up of a number of convolutional layers that, as they go, progressively bring down the spatial resolution of the input picture while simultaneously bringing up the total number of feature mappings. The expanding route is made up of a number of convolutional layers that, as they go, increasingly raise the level of spatial resolution of the output while simultaneously lowering the total number of feature

mappings. The Residual U-Net incorporates, in addition to these regular U-Net layers, residual connections between the levels in the contracting route and the equivalent layers in the expanding path. The network may skip over sections of the convolutional layers because of these residual connections, which helps to resolve the vanishing gradient problem and improves the network's accuracy.

#### 3.2.1 Residue Block

The residual block is a key component of the ResNet design, which addresses the issue of vanishing gradients in extremely deep neural networks. A residual block has one or more convolutional layers and element-wise addition of the input to the output. Traditional feedforward neural networks use the output of the preceding layer as input, apply a nonlinear activation function, and generate a new output. The gradient signal backpropagated across layers may become extremely tiny as the network becomes deeper, making training challenging. Vanishing gradient issue.

The residual block helps to mitigate the vanishing gradient problem by introducing a shortcut connection, or skip connection, that allows the network to directly propagate the input through the block. The residual block computes the difference between its input and output and adds it to its input. This means that the output of the block is the sum of the residual mapping and the input, rather than just the output of the convolutional layers. The addition of the input to the output of the convolutional layers creates a direct path for the gradient signal to flow through the block, which makes it easier to train deep networks. This is because the gradient signal has a shorter path to travel, so it is less likely to become small or vanish.

The Residue block of the proposed model has the following layers:

Convolution Layer: Convolutional layers in computer vision models perform convolution by sliding filters across input images, calculating dot products with local areas to learn spatially invariant features for pattern recognition. Unlike fully connected layers, which disregard spatial relationships, convolutional layers detect patterns across input data, crucial for image analysis in deep learning architectures.

Batch Normalization Layer: Batch normalization normalizes inputs to each layer in deep neural networks, enhancing training and network performance. It computes mean and standard deviation over small batches, then normalizes inputs. Gamma and beta parameters enable learnable scaling and shifting of normalized inputs, optimizing network performance.

ReLU Activation: The rectified linear unit (ReLU) is a widely used activation function in deep learning, defined

as  $f(x) = \max(0, x)$ , returning  $x$  if positive, zero otherwise. It introduces crucial non-linearity for the network to learn complex relationships between inputs and outputs. Without it, the network would be limited to representing linear functions, hindering its capacity for complexity.

**Addition layer:** An addition layer performs element-wise addition between input tensors, adding corresponding values to produce an output tensor. Commonly found in models with residual connections like ResNet, it adds output from a residual block to its input, aiding in learning residual functions and potentially enhancing network performance.

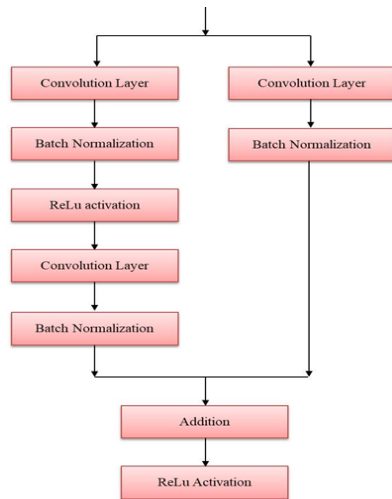


Fig. 1. Residue block

### 3.2.2 UP-Sampling Block

In deep learning, upsampling block refers to a set of operations that increase the spatial resolution of feature maps. Upsampling is often used in tasks such as image segmentation, where high-resolution feature maps are required to accurately localize objects within an image.



Fig. 2. Proposed Residual U-Net model

Figure 2 shows the proposed Residual U-Net model. The model begins with an input layer which reads the input images. After this layer comes two sets of convolution layers, then two sets of batch normalization layers come after that. Batch normalization is linked to three different sets of residual blocks as well as the maximum pooling layer. The maximum pooling layer receives the output of the residual block as its input. In each set

**Max pooling layer:** Max pooling reduces the number of parameters in the network by reducing the spatial size of the feature maps, which helps prevent overfitting by reducing the complexity of the model. It is also translation invariant, meaning that it will produce the same output for an object regardless of where it appears in the image. This can be useful for tasks such as object detection, where the location of an object in an image is not known in advance. Max pooling can also make the model more robust to small translations or distortions in the input image. This is because the maximum value in each pooling window is likely to remain the same even if the image is slightly shifted or distorted. It is computationally efficient, as it reduces the spatial size of the feature maps and reduces the number of parameters that need to be learned by the model. The fourth residual block is connected to four sets of up-sampling and residue blocks. Finally, the model contains a convolution layer.

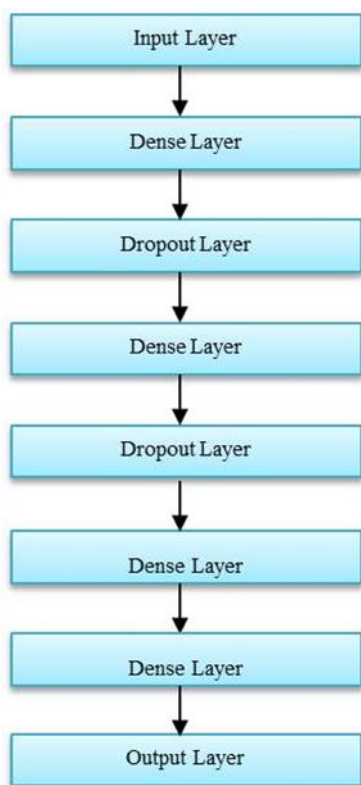
### Focal Tversky loss function:

The Focal Tversky loss function is often used in deep learning tasks that include semantic segmentation, serving as a modified form of the Tversky loss function. The Focal Tversky loss function is specifically developed to tackle the problem of class imbalance in segmentation tasks, when there is a substantial disparity in the number of pixels belonging to different classes. The Focal Tversky loss function extends the Tversky loss function by introducing a weighting factor that puts more emphasis on hard-to-classify pixels. The Focal Tversky loss function places more emphasis on hard-to-classify pixels by assigning them a higher weight in the loss function. This can help the model to focus on the most important pixels in the image and improve the overall performance of the segmentation task.

### CNN model for Brain Tumor Stage classification:

The CNN model presented for categorizing the stages of brain tumors consists of many layers, which are standard elements of deep learning models. The first layer is referred to as the input layer, and its primary function is to receive and process all of the data. For brain stage classification, the input consists of brain scans that depict different stages of brain tumor progression. size and form of the data that is being fed into the system will determine the dimensions of the input layer. The layer that comes

after the input layer is a Dense layer, which is also referred to as a completely linked layer. This layer establishes synaptic connections between all the neurons in the layer directly below it and all the neurons in the layer directly above it. For brain tumor stage classification, the thick layer plays a crucial role in capturing intricate patterns and connections among various variables in the input data. It is a very important part of the process of obtaining useful information from the input. Following the first dense layer is a dropout layer, which is included because its presence helps avoid overfitting. Regularization strategies like dropout are often used in deep learning models. During the training process, the dropout algorithm will arbitrarily change a percentage of the input units to zero at each update. This will assist in avoiding the model from becoming too dependent on a small subset of neurons. This layer enhances the model's ability to generalize new information by reducing the risk of overfitting. The CNN model developed for classifying the stage of brain tumors is shown in Figure 3.



**Fig. 3.** CNN model architecture for Brain tumor stage classification

Following the initial dropout layer comes a subsequent dense layer that keeps on extracting and learning increasingly sophisticated representations from the output of the layer before it. This layer contributes to the further capture of relevant patterns and characteristics within the data. It provides the model with more depth, which in turn enables it to learn more complex representations. After adding the second dense layer, the next step is to add the second dropout layer. This is done to further regularize the

model. This dropout regularization is applied to the output of the dense layer in a manner that is analogous to the dropout layer that came before it. It aids in preventing overfitting and improving the model's generalization ability. The model becomes more resilient as a result of the random elimination of units, making it less likely to depend on certain aspects of the data.

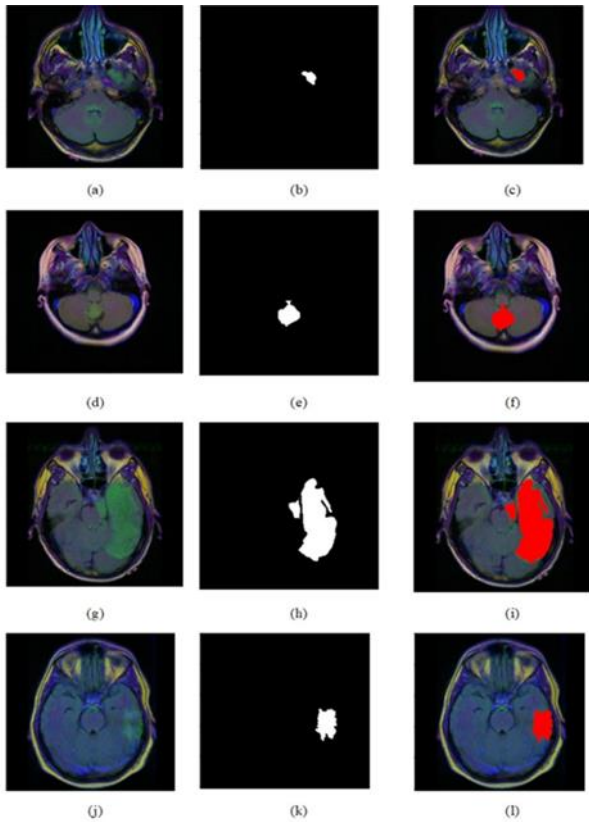
Following the output of the second dropout layer comes the third dense layer, which is responsible for further processing of the information and the extraction of higher-level representations from the output of the dropout layer that came before it. Each dense layer introduces non-linear transformations to the data, enabling the model to learn complex mappings. Because of the extra thick layer, the model is able to acquire more abstract representations, which enables it to capture higher-level characteristics linked to the categorization of brain stages. After the third dense layer, a third dropout layer is added to the model so that it may be regularized even more. This last dropout layer contributes to lowering the likelihood of the model overfitting to the data by boosting its ability to perform on data that has not yet been seen. It is complementary to the dropout layers that came before it, and it adds an extra degree of regularization to the model, which helps to improve its capacity for generalization. The ultimate results of classification are produced by the output layer of the CNN model, which serves as the last layer. When classifying brain stages, the output layer could be made up of neurons that correspond to the various stages of the brain.

The model may acquire hierarchical representations of the input data by arranging dense layers together with dropout layers. This allows the model to capture both low-level and high-level elements that are significant for brain stage categorization. The dropout layers help to regularize the model and prevent it from being overfit, which ultimately improves the model's capacity to generalize to data that has not yet been observed. It is crucial to note that the model's particular architecture and parameters may need to be modified via testing and validation in order to attain optimum performance for the brain stage classification task. After the CNN model has been trained, it is tested on a dataset to see how well it performs in identifying the stages of brain tumours.

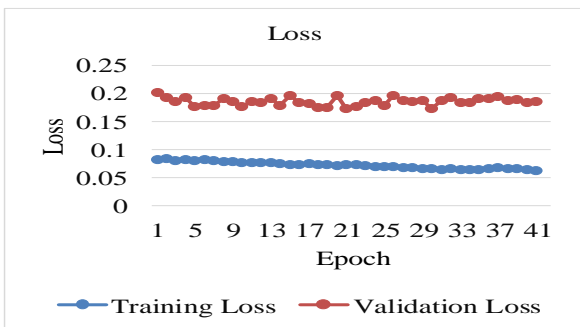
In conclusion, the integration of dense and dropout layers in a CNN model facilitates the extraction of meaningful features and regularizes the learning process. This architectural approach is instrumental in enabling the model to perform complex tasks such as brain stage classification with high accuracy and robustness. The process of fine-tuning and validation ensures that the model is optimized for the specific application, leading to better performance and generalization capabilities.

#### 4. Experimental Analysis

The figure 4 shows the images in the dataset [16]. Figure (a), (d), (g), and (i) show the input MRI images, the ground truth mask is shown in (b), (e), (h), and (k) and the overlapped images are shown in (c), (f), (i) and (l).



**Fig.4.** Input database images

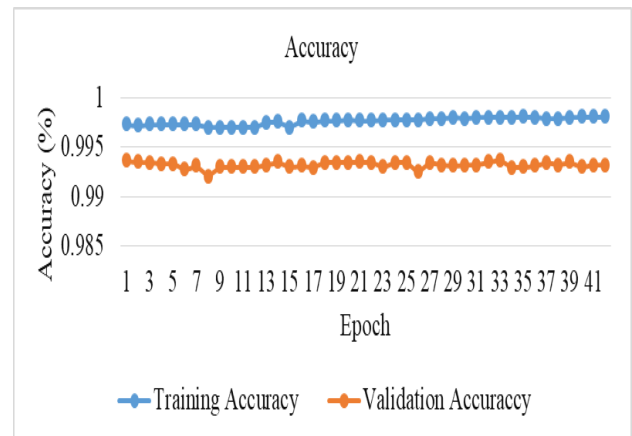


**Fig.5.** Training and Validation loss

Figure 5 displays the training as well as validation loss. Training loss as well as validation loss are often used metrics to evaluate the effectiveness of a model throughout the training process. Training loss is calculated as the discrepancy between the predicted output of a model and the actual output during the training phase. To put it another way, it assesses how well the model fits the training set of data. The training loss normally lowers over time as the model learns and becomes better. As opposed to training loss, validation loss quantifies the mistake or disagreement between a model's anticipated output and the actual output on a different dataset. The validation set is

the common name for this dataset. The validation loss is employed to assess the model's capacity to generalize to novel, untested data and to detect overfitting. Overfitting occurs when a model gets too complex and attempts to match the noise present in the training data, leading to poor generalization performance.

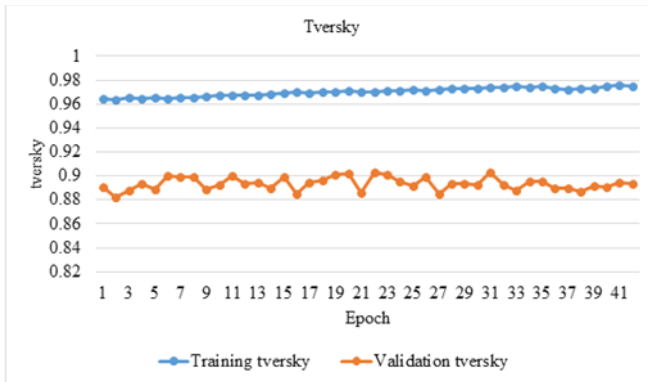
The goal during training is to minimize both the training and validation loss. However, it is important to monitor the validation loss carefully, as it is a better indicator of the model's generalization performance on new data. If the validation loss starts to increase while the training loss is still decreasing, it is a sign that the model is overfitting and adjustments need to be made to the model architecture or training process.



**Fig. 6.** Training and validation accuracy

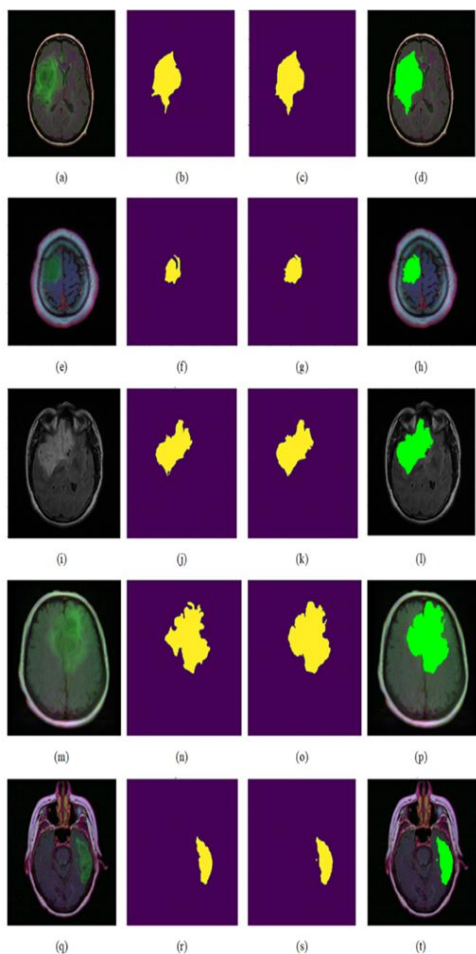
In machine learning, training accuracy and validation accuracy are two often used measures to assess how well a model performs during training. The training and validation accuracy are shown in Figure 6. The proportion of accurately anticipated outputs from a model using training data is known as training accuracy. To put it another way, it assesses how well the model fits the training set of data. The training accuracy often rises as the model develops and becomes better over time.

Validation accuracy, in contrast, quantifies the proportion of accurately predicted outcomes by a model using an independent dataset that wasn't utilized during the training process. The dataset is often known as the validation set. To assess the model's ability to apply its knowledge to fresh, untested data and identify overfitting, we use the validation accuracy. Overfitting occurs when a model becomes too complex and starts to fit the noise present in the training data, leading to poor generalization performance.



**Fig. 7.** Training and validation Tversky

Fig.7 depicts the training as well as the validation performed by Tversky. In binary image segmentation tasks, these are the metrics that are used to assess the performance of a classification model. The Tversky index is a similarity measure that evaluates the overlap between two sets. It is often used in medical picture segmentation jobs because of its accuracy and reliability. The objective of binary image segmentation is to separate a picture into two distinct areas called the foreground and the background. Training and validation Tversky are used in order to quantify the degree of similarity that exists between the segmentation that was anticipated and the segmentation that really occurred.



**Fig. 8.** Predicted masks

Fig.8 shows the obtained results of the proposed model. Images (a), (e), (i), (m) and (q) shows the input images. (b), (f), (j), (n) and (r) show the actual tumor mask. (c), (g), (k), (o) and (s) show the predicted output mask. (d), (h), (l), (p) and (t) show the predicted mask overlapped MRI image.

**Table 1.** Comparative analysis

	<i>MSE</i>	<i>PSNR</i>	<i>Tversky</i>
Unet	152.78	26.29	0.71
Unet++	91.24	28.52	0.75
Proposed Residual Unet	56.75	30.59	0.89

Form Table.1, the Unet model's MSE was 152.78. MSE indicates model accuracy. The Unet model's PSNR is 26.29, which quantifies the ratio between the maximum signal power and the image-degrading noise power. Image quality increases with PSNR. The Unet model also had a Tversky score of 0.71, which measures the overlap between predicted and ground truth pictures. Similarity increases as Tversky scores approach 1. MSE was 91.24 for the Unet++ model, which was more accurate than Unet. Compared to Unet, Unet++ has a PSNR of 28.52, improving picture quality. The Unet++ model has a Tversky score of 0.75, showing greater overlap and similarity between predicted and ground truth pictures. The Proposed Residual Unet model predicted target images with the lowest MSE, 56.75. This model has 30.59 PSNR, suggesting great picture quality. The Proposed Residual Unet framework has the highest Tversky score of 0.89, indicating a significant level of overlap as well as similarity between the predicted and ground truth images. Based on the evaluation measures, the Proposed Residual Unet model beats the Unet and Unet++ models in accuracy, picture quality, and ground truth image similarity. These findings show that the Proposed Residual Unet model may be more effective and accurate for picture segmentation or reconstruction.

The proposed CNN framework for classifying brain tumor stage makes accurate use of cutting-edge deep learning methods. To capture complex patterns and connections in the input data, the model uses numerous layers, including dense layers and dropout layers. The model learns to extract useful characteristics from brain tumor images via training and optimization. The proposed model achieves good accuracy and performance in properly identifying brain tumor stages by using the capabilities of convolutional neural networks. This approach has a lot of potential for helping doctors identify and treat brain cancers by facilitating early diagnosis and the right therapies for better patient outcomes.



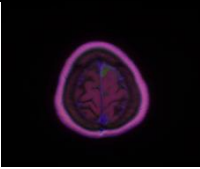

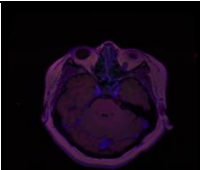
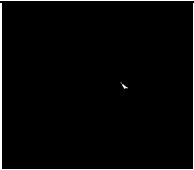
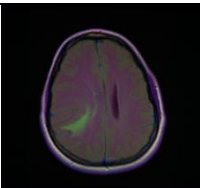

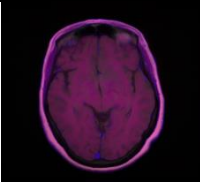
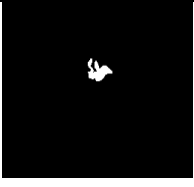
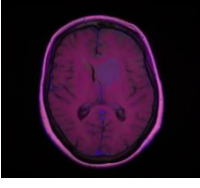

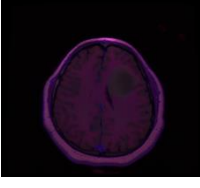
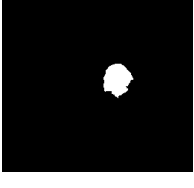
**Table 2.** Confusion Matrix

	<i>Stage 1</i>	<i>Stage 2</i>	<i>Stage 3</i>	<i>Stage 4</i>
Stage 1	112	10	1	0
Stage 2	12	108	5	3
Stage 3	0	3	115	4
Stage 4	1	4	4	118

Table 2 displays the confusion matrix of a classifier on four brain tumor stages. Table rows show actual phases, whereas columns show expected stages. The table shows the number of successfully categorized occurrences. 112 cases were accurately categorised as stage 1 in the first

row, first column of table 3. 10 cases in the first row, second column were stage 1 but misclassified as stage 2. Based on findings from Table 2, the proposed CNN model achieved 91% accuracy. The informative overview of numerous performance measures for different brain tumor stages can be seen in Table 4. These metrics provide an all-encompassing insight of the model's ability to appropriately categorize cases across a variety of classifications.

**Table 3** Brain Tumor Classification results

<b>Original Image</b>	<b>Mask Image</b>	<b>Area</b>	<b>Distance</b>	<b>Classification</b>
		205	23.701114	<b>Stage-1</b>
		109	59.811258	<b>Stage-1</b>
		601	49.865218	<b>Stage-2</b>
		545	25.885965	<b>Stage-2</b>
		1242	20.924390	<b>Stage-3</b>
		1316	27.055051	<b>Stage-3</b>

		2211	28.958750	<b>Stage-4</b>
		2554	30.741186	<b>Stage-4</b>

The suggested CNN model-based categorization of brain tumors is discussed in table.3. The original brain tumor picture and its corresponding mask image in the first row have an area of 205 and a distance of 23.701114. The categorization of the brain tumor is found to be Stage-1 based on these data. The next rows in table 3 provide the same data for various original and mask pictures. In a similar manner, Stage-3 is produced by the third and fourth rows, which depict the original and mask pictures with various regions and distances. The fifth and sixth rows both follow this pattern, with Stage-4 classifications determined by the original and mask pictures' respective areas and distances.

**Table 4** Classification report of the proposed model

Stage	Precision	Recall	Sensitivity	F1 score
Stage 1	0.896	0.910	0.910	0.903
Stage 2	0.857	0.844	0.844	0.850
Stage 3	0.935	0.943	0.943	0.939
Stage 4	0.929	0.929	0.929	0.929
<b>Accuracy</b>	<b>91%</b>			

Precision, recall, sensitivity and the F1 score assess every stage, giving an overall overview of the model's classification capabilities. The model predicts Stage 1 cases 89.6% of the time with an accuracy of 0.896. The model's recall score of 0.910 shows it can catch 91.0% of Stage 1 occurrences, resulting in a well-balanced F1 score of 0.903. Stage 2's precision is 0.857, representing 85.7% instance classification accuracy. The model correctly identified 84.4% of Stage 2 instances, resulting in an F1 score of 0.850 that shows its balanced predictions. Stage 3's precision score of 0.935 indicates the model's 93.5% accuracy in classifying Stage 3 events. The model's F1 score of 0.939 comes from its ability to identify 94.3% of Stage 3 occurrences with a recall of 0.943. Stage 4 predicts cases with 92.9% accuracy and a precision score of 0.929. The model consistently identifies 92.9% of Stage 4

instances with a recall score of 0.929. This level balances accuracy and recall with an F1 score of 0.929.

## 5. Conclusion

Automated brain tumor segmentation and identification refers to the use of machine learning and computer vision methods to automatically identify and divide brain tumors in medical pictures, namely magnetic resonance imaging (MRI) scans. This procedure is crucial for precise and effective detection of brain tumors, which may be hard to recognize and pinpoint without the aid of specialized tools. The Residual U-Net (Res-U-Net) is an altered version of the U-Net design that integrates residual connections. These connections facilitate the network in acquiring more intricate representations of the input data and provide several advantages in brain tumor segmentation. Residual connections facilitate the training of deeper networks and alleviate the issue of disappearing gradients. As a result, Res-U-Net can achieve higher accuracy in brain tumor segmentation, especially for small or complex tumors. Res-U-Net requires fewer iterations to converge than traditional U-Net architecture. This led to faster training times and more efficient use of computational resources. Res-U-Net is robust to variations in input data, such as differences in image quality or orientation. This is crucial in medical imaging, where image quality can vary widely depending on factors such as patient movement or scanner settings. The proposed model produced a higher PSNR of 30 and better Tversky of 0.89.

## References

- [1] Arabahmadi, Mahsa, Reza Farahbakhsh, and Javad Rezazadeh. "Deep learning for smart Healthcare—A survey on brain tumor detection from medical imaging." *Sensors* 22, no. 5 (2022): 1960.
- [2] Arif, Muhammad, F. Ajesh, Shermin Shamsudheen, Oana Geman, Diana Izdrui, and Dragos Vicoveanu. "Brain tumor detection and classification by MRI using biologically inspired orthogonal wavelet transform and deep learning techniques." *Journal of Healthcare Engineering* 2022 (2022).
- [3] Sharma, Arpit Kumar, Amita Nandal, Arvind Dhaka,

- Deepika Koundal, Dijana Capeska Bogatinoska, and Hashem Alyami. "Enhanced watershed segmentation algorithm-based modified ResNet50 model for brain tumor detection." *BioMed Research International* 2022 (2022).
- [4] Chattopadhyay, Arkapravo, and Mausumi Maitra. "MRI-based brain tumor image detection using CNN based deep learning method." *Neuroscience Informatics* (2022): 100060.
- [5] Soomro, Toufique A., Lihong Zheng, Ahmed J. Afifi, Ahmed Ali, Shafiullah Soomro, Ming Yin, and Junbin Gao. "Image segmentation for MR brain tumor detection using deep learning: A Review." *IEEE Reviews in Biomedical Engineering* (2022).
- [6] Arunkumar, N., Mazin Abed Mohammed, Mohd Khanapi Abd Ghani, Dheyaa Ahmed Ibrahim, Enas Abdulhay, Gustavo Ramirez-Gonzalez, and Victor Hugo C. de Albuquerque. "K-means clustering and neural network for object detecting and identifying abnormality of brain tumor." *Soft Computing* 23 (2019): 9083-9096.
- [7] Lather, Mansi, and Parvinder Singh. "Investigating brain tumor segmentation and detection techniques." *Procedia Computer Science* 167 (2020): 121-130.
- [8] Sheela, C. Jaspin Jeba, and G. J. M. T. Suganthi. "Morphological edge detection and brain tumor segmentation in Magnetic Resonance (MR) images based on region growing and performance evaluation of modified Fuzzy C-Means (FCM) algorithm." *Multimedia Tools and Applications* 79 (2020): 17483-17496.
- [9] Shemanto, Tanber Hasan, Lubaba Binte Billah, and Md Abrar Ibtesham. "A Novel Method of Thresholding for Brain Tumor Segmentation and Detection." In *Proceedings of International Conference on Information and Communication Technology for Development: ICICTD 2022*, pp. 277-289. Singapore: Springer Nature Singapore, 2023.
- [10] Thaha, M. Mohammed, K. Pradeep Mohan Kumar, B. S. Murugan, S. Dhanasekeran, P. Vijayakarthick, and A. Senthil Selvi. "Brain tumor segmentation using convolutional neural networks in MRI images." *Journal of medical systems* 43 (2019): 1-10.
- [11] Liu, Zhihua, Lei Tong, Long Chen, Zheheng Jiang, Feixiang Zhou, Qianni Zhang, Xiangrong Zhang, Yaochu Jin, and Huiyu Zhou. "Deep learning based brain tumor segmentation: a survey." *Complex & Intelligent Systems* (2022): 1-26.
- [12] Amin, Javeria, Muhammad Sharif, Mussarat Yasmin, Tanzila Saba, Muhammad Almas Anjum, and Steven Lawrence Fernandes. "A new approach for brain tumor segmentation and classification based on score level fusion using transfer learning." *Journal of medical systems* 43 (2019): 1-16.
- [13] Ghosh, Sourodip, Aunkit Chaki, and K. C. Santosh. "Improved U-Net architecture with VGG-16 for brain tumor segmentation." *Physical and Engineering Sciences in Medicine* 44, no. 3 (2021): 703-712.
- [14] Thillaikkarasi, R., and S. Saravanan. "An enhancement of deep learning algorithm for brain tumor segmentation using kernel based CNN with M-SVM." *Journal of medical systems* 43 (2019): 1-7.
- [15] Shivhare, Shiv Naresh, Nitin Kumar, and Navjot Singh. "A hybrid of active contour model and convex hull for automated brain tumor segmentation in multimodal MRI." *Multimedia Tools and Applications* 78, no. 24 (2019): 34207-34229.
- [16] <https://www.kaggle.com/datasets/mateuszbuda/lgg-mri-segmentation>
- [17] B. Anilkumar, P. Rajesh Kumar, –Multi brain tumor classification in MR brain images through transfer learning model, *Journal of Applied science and computations (JASC)* 7 (May 2020) 41–49.

1. **Author1:** Murali Krishna Atmakuri,

muralikrishna.atmakuri80@gmail.com

Research Scholar, Department of Electronics and Instrumentation Engineering, Faculty of Engineering and Technology, Annamalai University, Annamalinagar, India

2. **Author2:** A. Ganesh Ram

agram72@gmail.com

Department of Instrumentation Engineering, Madras Institute of Technology, Anna University, Chennai, India

3. **Author3:** V.V.K.D.V. Prasad

varaprasadvkd@gmail.com

Department of Electronics and Communication Engineering, Gudlavalleru Engineering College, Gudlavalleru, India